Abstract

The increasing adoption of renewable energy sources necessitates efficient and reliable methods for integrating them into the existing AC grid infrastructure. Non-isolated high gain DC-DC converters have emerged as vital components in this integration process, facilitating the seamless transfer of power between renewable sources and the grid. This paper proposes a novel non-isolated high gain DC-DC converter design optimized for interfacing renewable energy systems with the AC grid. The proposed non-isolated high gain DC-DC converter presents a promising solution for the seamless integration of renewable energy systems with the AC grid. Its compact design, high efficiency, and grid-friendly features make it well-suited for various applications, ranging from residential solar installations to large-scale renewable energy plants. In this paper, a nonisolated high gain dc–dc converter is proposed without using the voltage multiplier cell and/or hybrid switched-capacitor technique. The proposed topology utilizes two nonisolated inductors that are connected in series/parallel during discharging/charging mode. The operation of switches with two different duty ratios is the main advantage of the converter to achieve high voltage gain without using extreme duty ratio.

Contents

List of Tables

List of Figures

Chapter 1

Introduction

1.1 Introduction to DC-DC converters

DC-DC converters are essential components in modern power electronics, responsible for converting one level of direct current (DC) voltage to another. They are widely used in a variety of applications, including renewable energy systems, electric vehicles, consumer electronics, and industrial power supplies. The primary function of a DC-DC converter is to step up (boost) or step down (buck) the input voltage to meet the requirements of the load or to interface with other components in the system.

In many electrical systems, the power source and the load operate at different voltage levels. For instance, batteries and photovoltaic (PV) panels typically produce low-voltage DC power, while electronic devices, motors, and grid-tied inverters often require higher or different voltage levels. DC-DC converters provide the necessary voltage transformation, allowing for efficient energy transfer between the source and the load. They also play a crucial role in improving the efficiency, reliability, and performance of power systems by regulating output voltage, minimizing losses, and protecting sensitive components.

DC microgrid technology is advancing with the increasing integration of distributed generation sources. Since DC power generators typically produce low output voltages, there is a significant need for highly efficient DC-DC converters [1],[2]. While the traditional non-isolated boost converter remains the preferred choice for this task, its efficiency is constrained at high duty cycle values. To overcome this limitation and enhance the conversion ratio, numerous studies have explored various alternative topologies as potential solutions for these applica-

tions. Today, high gain DC-DC converters are employed in a broad range of applications, such as battery backup systems for uninterruptible power supplies, load of high-intensity discharge lamps in automobile headlamps, electric traction systems, and certain medical devices. [3]- [5]. Traditionally, conventional DC-DC boost converters have been used to increase voltage levels. Moreover, selecting large duty ratios to obtain higher voltage gains not only intensifies these conduction losses [6]-[9].

To achieve a high output voltage, traditionally, multiple conventional boost converters need to be connected as shown in fig. 1.1 However, with this innovative high-gain DC-DC boost converter, we can minimize the number of devices required as shown in fig. 1.2. Numer-

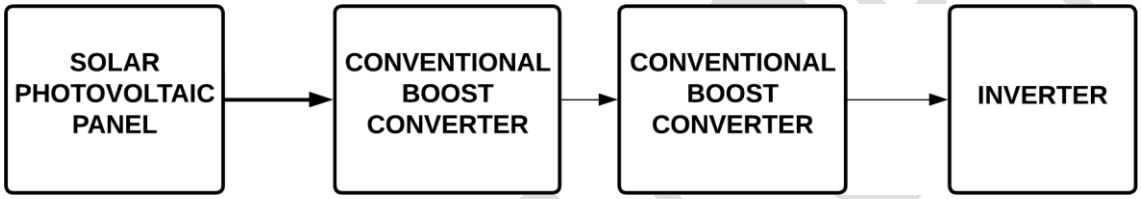

Figure 1.1: System with conventional converter

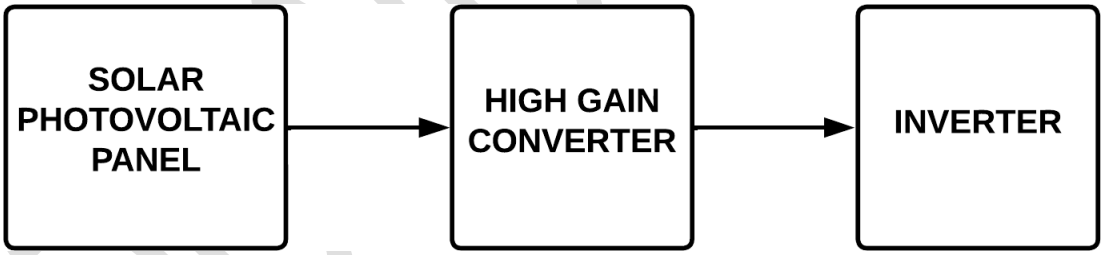

Figure 1.2: System with high gain converter

ous isolated DC-DC converter designs have been suggested in academic and industry research to secure the necessary high voltage gain . However, these designs frequently encounter issues such as transformer core saturation. Consequently, where galvanic isolation is not a requirement, non-isolated DC-DC converters present a viable alternative, offering high voltage gains while also minimizing both size and cost [10]-[12]. At times, turns ratio of coupled inductor is elevated to attain the intended voltage conversion ratio, leading to high input current ripple.

Consequently, the utilization of an input filter becomes important to minimize this current ripple [13]-[20].

1.2 Literature Reported

Researchers propose a distributed control strategy that does not rely on a central controller, making the system more robust and scalable. Each storage unit in the micro-grid operates autonomously, making decisions based on local measurements and predefined rules. The control strategy ensures that the state of charge (SoC) of all storage devices is maintained within safe limits, and the power balance of the micro-grid is preserved. The approach is designed to optimize the use of renewable energy, reduce losses, and enhance the reliability and stability of the micro-grid [1].

Different converter topologies are reviewed, including inverters, DC-DC converters, and AC-DC converters. The paper categorizes these topologies based on the type of RES and the specific application, such as grid-connected or stand-alone systems. The paper highlights various control strategies for power-electronic converters, focusing on their ability to manage power flow, ensure grid stability, and enhance system efficiency. These strategies include voltage control, current control, and maximum power point tracking (MPPT) [2].

The paper provides a detailed mathematical model for the boost converter's voltage-loop transfer function, factoring in MOSFET switching characteristics. The reseachers emphasize the effects of MOSFET delay on the system's dynamic performance, demonstrating how the delay influences the stability and response of the voltage loop. Their results highlight that incorporating MOSFET delay into the design improves the accuracy of transfer function analysis, which is crucial for optimizing the control system in high-frequency switching applications [3].

The researchers propose a new active clamp circuit to achieve Zero-Voltage Switching (ZVS), which minimizes switching losses by ensuring that the MOSFETs switch at zero voltage, improving efficiency in power converters. The paper presents a family of converters that utilize this active clamp ZVS cell. These converters are designed to work efficiently across a range of applications while maintaining ZVS across different operating conditions. The researchers offer a comprehensive analysis of the proposed ZVS converters, including the derivation of design equations and performance characteristics [4].

The paper categorizes and reviews different non-isolated high-gain DC-DC converter topolo-

gies, including: Cascaded Boost Converters, Coupled Inductor-Based Converters, Switched Capacitor Converters, Quadratic Boost Converters, Interleaved Boost Converters, Each topology is analyzed in terms of its voltage gain, efficiency, component count, and complexity [5].

The paper introduces a line-interactive UPS system that provides backup power and enhances the reliability of microgrids, especially in the presence of grid disturbances or blackouts. The paper focuses on the role of the UPS in regulating voltage and frequency in the microgrid, ensuring stable power quality whether the microgrid is connected to the main grid or operating independently [6].

The paper reviews different battery charger topologies, including both on-board and off-board chargers. The researchers discuss different charging power levels, ranging from Level 1 (slow charging) to Level 3 (fast charging), and the implications for charging time, vehicle range, and the overall efficiency of the electric vehicle charging process [7].

The researchers propose two new transformerless DC-DC converter topologies that provide high step-up voltage gain, making them suitable for applications such as renewable energy systems, where high voltage is required from low voltage sources like photovoltaic panels or fuel cells. The key innovation in these converters is the integration of coupled inductors and voltage multiplier cells, which significantly boost the output voltage while maintaining high efficiency and low voltage stress across the components [8].

The paper present a novel bidirectional DC-DC converter designed to facilitate efficient power transfer in both directions, making it suitable for applications requiring energy storage and retrieval, such as battery management systems and renewable energy systems. The proposed converter features a unique circuit topology that integrates the advantages of both buck and boost converters, allowing it to operate effectively in both charging and discharging modes [9].

The researchers present a novel high step-up DC-DC converter that integrates coupled inductor and switched-capacitor techniques to enhance voltage gain. This innovative converter addresses the challenges associated with traditional high-gain converters, such as high component stress and reduced efficiency [10].

Introduces a new design for a DC-DC step-up (boost) converter that employs a switched-coupled inductor technique. The proposed converter offers high voltage gain with improved efficiency, addressing limitations in traditional boost converters, particularly for low-voltage renewable energy sources like photovoltaic systems. The researchers also derive several vari-

ations of the core design to meet different application requirements. This innovative approach enhances power conversion efficiency while minimizing the size and cost of the converter, making it highly suitable for industrial and renewable energy applications [11].

The paper presents a high step-up DC-DC converter that combines coupled inductor and switched capacitor techniques. The proposed design uses a single-switch configuration, which simplifies the control system and reduces cost while achieving a high voltage gain. The converter operates in quasi-resonant mode, minimizing switching losses and improving overall efficiency [12].

This paper introduces a new design for a quadratic boost converter that operates with a quasi-resonant technique. This design integrates a single resonant network to achieve soft switching, reducing switching losses and electromagnetic interference (EMI). The quadratic boost converter provides a higher voltage gain compared to traditional boost converters, making it ideal for high-voltage applications. The paper presents both theoretical analysis and experimental results, showcasing the improved efficiency and performance of the converter in industrial power systems [13].

The paper provides a comprehensive review of non-isolated high-voltage step-up DC-DC converter topologies derived from the traditional boost converter. The researchers categorize and analyze various designs, highlighting their operational principles, advantages, and limitations. The survey emphasizes the importance of these converters in applications such as renewable energy systems, where efficient voltage boosting is essential. Additionally, the paper discusses key performance metrics, including efficiency, voltage gain, and component count, while also identifying trends and future research directions in the field of high-voltage DC-DC conversion [14].

The paper outline a high-voltage pulse generator that leverages a DC-to-DC boost converter combined with capacitor-diode voltage multipliers to achieve high voltage outputs necessary for bacterial decontamination applications. The design utilizes a boost converter to step up the input voltage and capacitor-diode multipliers to further increase the voltage, generating high-voltage pulses suitable for the targeted application [15].

The paper shows a novel high step-up boost converter designed to achieve significant voltage gain while maintaining high efficiency. The proposed converter incorporates a passive lossless clamp circuit, which effectively mitigates voltage spikes and reduces switching losses [16].

This chapter provides a comprehensive overview of different converter topologies, including DC-DC converters, AC-DC converters, and DC-AC inverters. Rashid discusses the operational principles, advantages, and limitations of each topology, along with practical considerations for their design and implementation. The chapter also covers key concepts such as control strategies, efficiency, and thermal management [17].

Paper introduces innovative converter designs that integrate switched-capacitor and switched-inductor techniques to create transformerless hybrid DC-DC PWM converters. The paper includes theoretical analyses, simulations, and experimental results, demonstrating the effectiveness of the proposed designs in achieving high performance without the need for transformers [18].

The Paper focuses on the development of a high voltage gain boost converter that employs coupled inductors. By utilizing coupled inductors, the converter effectively reduces voltage stress on the components and improves performance in high-voltage applications [19].

The paper presents a novel interleaved DC-DC converter designed for high voltage gain applications. The proposed converter features a common active clamp circuit, which enhances efficiency by reducing switching losses and providing soft switching conditions for the power switches. The interleaved design helps to distribute the input current, thereby minimizing input ripple and improving overall performance [20].

The study discusses the design of a nonisolated DC-DC converter specifically aimed at high gain applications in DC microgrids. The researchers propose a converter topology that enhances voltage conversion while maintaining high efficiency and reducing component stress. By leveraging advanced techniques such as coupled inductors and switched-capacitor methodologies, the converter effectively meets the demands of DC microgrids, where efficient power management is crucial. The paper includes detailed theoretical analysis, simulation results, and experimental validation, demonstrating the converter's capability to provide stable and high voltage output, making it suitable for renewable energy integration and energy storage applications in microgrid systems [21].

1.3 Motivation

The global energy landscape is undergoing a significant transformation, driven by the urgent need to reduce greenhouse gas emissions and mitigate the impacts of climate change. Renew-

able energy sources such as solar, wind, and fuel cells have emerged as critical components of this transition, offering sustainable alternatives to fossil fuels. However, the effective integration of these renewable sources into existing power systems, particularly the AC grid, poses several technical challenges. One of the key challenges is the variability and typically low voltage output of renewable energy sources, which necessitates efficient and reliable power conversion solutions.

DC-DC converters play a pivotal role in this context by stepping up the low voltage generated by renewable sources to higher levels suitable for grid interfacing and energy storage. Traditional isolated DC-DC converters, while providing necessary electrical isolation, are often complex, bulky, and less efficient. These drawbacks limit their scalability and cost-effectiveness in large-scale renewable energy systems, where efficiency, compactness, and cost are critical considerations.

The motivation behind exploring non-isolated high gain DC-DC converters lies in their potential to overcome these limitations. Non-isolated converters, by eliminating the need for isolation transformers, can achieve higher efficiency, reduced size, and lower cost, making them more suitable for renewable energy applications where isolation is not a critical requirement. Moreover, the ability to achieve high voltage gain with simplified circuitry opens up new possibilities for enhancing the performance and integration of renewable energy systems.

This research is motivated by the need to develop innovative power conversion solutions that address the unique challenges posed by renewable energy integration. By focusing on non-isolated high gain DC-DC converters, this thesis aims to contribute to the advancement of power electronics technologies that are essential for enabling the widespread adoption of renewable energy. The results of this research are expected to play an important role in shaping how future energy systems are designed and operated, helping the world move towards more sustainable and reliable energy solutions.

1.4 Problem Description and objectives

In the integration of renewable energy sources (such as solar photovoltaic systems and wind turbines) with the AC grid, efficient energy conversion is critical. Renewable energy sources often generate DC power at varying voltage levels, which needs to be converted to a higher voltage DC to match the AC grid's voltage requirements or for energy storage systems. Tradi-

tional isolated DC-DC converters are not always suitable due to their complexity, size, and cost. Therefore, non-isolated high-gain DC-DC converters have become an attractive alternative, as they can efficiently step up the DC voltage without the need for isolation transformers. Renewable energy sources often produce low or intermediate DC voltages that need to be stepped up to higher voltage levels to match grid requirements or to interface with energy storage systems.

Achieving high voltage gain with high efficiency is challenging due to inherent limitations in conventional DC-DC converters. High-gain converters can suffer from efficiency losses due to high component stress, increased conduction losses, and switching losses. Maintaining high efficiency across a range of operating conditions is essential to ensure effective utilization of renewable energy. Non-isolated converters need to be designed to handle high voltage gains while minimizing the complexity of the circuitry and maintaining reliability. Components such as inductors and capacitors must be chosen carefully to manage voltage stress and ensure reliable operation. The converter must meet grid synchronization requirements, including voltage and frequency regulation, to ensure smooth integration with the AC grid. Develop and optimize non-isolated high-gain DC-DC converter topologies that can effectively step up DC voltages from renewable sources to the required levels for grid integration or energy storage. Focus on improving efficiency by minimizing losses and component stress. Ensure that the converter design meets the necessary grid compliance standards for voltage and frequency regulation. Develop control strategies that facilitate seamless integration with the AC grid, including synchronization and power factor correction.

Chapter 2

Novel Non-isolated High Gain DC-DC Converter

2.1 Introduction

The converter attain high voltage gain through the selection of appropriate duty cycles and the careful design of inductor and capacitor values. It boasts the following advantages: 1. The converter employs three power switches with two distinct duty ratios to attain a high voltage gain. 2. Inductor energy is efficiently delivered to the load without the need for additional clamping circuits. 3. The voltage gain achieved by the converter is better than conventional boost converters. 4. Voltage stress on the diodes and switches is minimized relative to the output voltage percentage. 5. The converter achieves substantial voltage gain without relying on voltage multiplier cells (VMCs) or hybrid switched-capacitor techniques [21].

2.2 Circuit Description

The circuit consists of:

Input voltage ($V\,in$),

Three active switches (Q_1, Q_2, Q_3),

Two inductors (L_a and L_b),

Two diodes (D_a and D_b),

One output capacitor (C),

Load resistor (R).

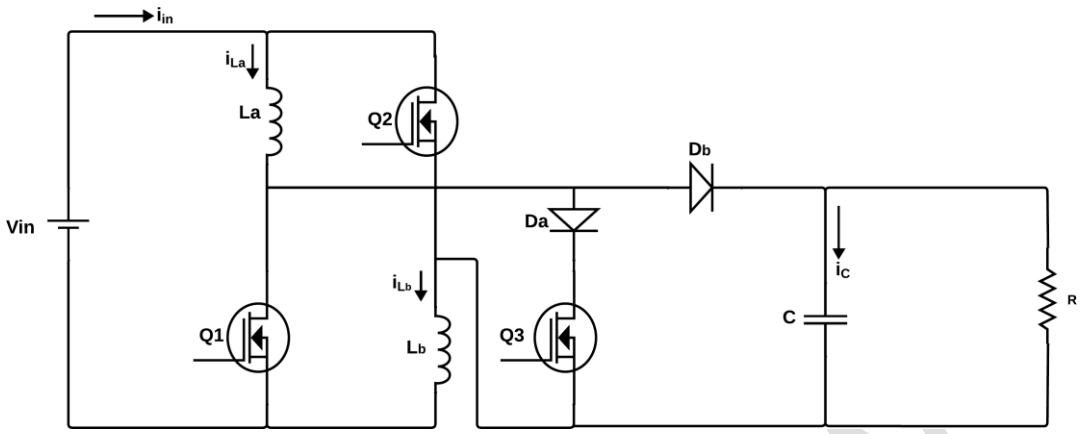

Figure 2.1: circuit diagram

a non-isolated high gain DC-DC converter with a capacity of 2000W, designed to step up the voltage from 70V to 700V. The converter needs to achieve a high voltage boost ratio of 10:1.

Ideal Components: All components within the circuit, including switches, diodes, inductors, and capacitors, are assumed to be ideal. This means there are no ON-state resistances in the switches, no forward voltage drops across the diodes, and no equivalent series resistance (ESR) in the inductors and capacitors.

Output Capacitance: The output capacitor C is assumed to be sufficiently large to ensure that the output voltage remains constant. This large capacitance effectively filters out voltage ripple, thereby stabilizing the output voltage despite variations in the load or input.

Additionally, it is assumed that both inductors L_a and L_b have an equal number of turns.

$$L_a = L_b = L \tag{2.1}$$

The voltage across inductors are specified as follows:

$$V_{L_a} = L_a \frac{di_{L_a}}{dt} = L \frac{di_{L_a}}{dt} \tag{2.2}$$

where i_{La} and i_{Lb} are the current through the inductors L_a and L_b respectively.

2.2.1 Voltage gain of the converter

V_o represents the output voltage and V_{in} indicates the input voltage of the converter. The voltage gain is determined using the state-space averaging method as follows:

$$\frac{V_o}{V_{in}} = \frac{1 + D_1}{1 - D_1 - D_2} \tag{2.3}$$

2.2.2 Voltage stress on diodes and switches

The voltage stress across diodes D_a and D_b, denoted as V_{D_a} and V_{D_b} respectively, is described as:

$$V_{D_a} = V_{in} = 70V \tag{2.4}$$

$$V_{D_b} = V_{in} + V_o = 770V \tag{2.5}$$

The voltage stress across switches Q_1, Q_2 and Q_3, denoted as V_{Q_1}, V_{Q_2} and V_{Q_3} respectively, is described as:

$$V_{Q_1} = V_{Q_2} = \frac{V_o + V_{in}}{2} = 385V \tag{2.6}$$

$$V_{Q_3} = V_o = 700V \tag{2.7}$$

2.2.3 Design of Inductor

The crucial inductance value needed to run the converter in Continuous Conduction Mode is calculated using the following equation:

$$L_a, L_b = \frac{V_{in} D_1}{\Delta I_L F_{sw}} \tag{2.8}$$

where V_{in} is input voltage, Δi_L is ripple current, F_{sw} is switching frequency and D_1 is duty ratio of switch Q_1 and Q_2. Considering 40% current ripple, the inductor value is 1.75 mH.

2.2.4 Selection of Capacitor

The crucial capacitance value needed to run the converter in Continuous Conduction Mode is calculated using the following equation:

$$C = \frac{I_o D_2}{\Delta V_c F_{sw}} \tag{2.9}$$

where I_o is output current, ΔV_c is ripple voltage, F_{sw} is switching frequency and D_2 is duty ratio of switch Q_3. Considering 5V voltage ripple, the capacitor value is 3.99μF.

2.3 Small signal modeling of system

2.3.1 Mode 1

$$V_{L_a} = V_{L_b} = V_{in} \tag{2.10}$$

$$\frac{di_{L_a}}{dt} = \frac{di_{L_b}}{dt} = \frac{di_L}{dt} = \frac{V_{in}}{L} \tag{2.11}$$

$$\frac{di_{V_c}}{dt} = \frac{-V_o}{RC} \tag{2.12}$$

$$A_1 = \begin{bmatrix} 0 & 0 \\ 0 & \frac{-1}{RC} \end{bmatrix} \begin{bmatrix} i_L \\ V_c \end{bmatrix} + \begin{bmatrix} \frac{1}{L} \\ 0 \end{bmatrix} V_{in} \tag{2.13}$$

2.3.2 Mode 2

$$V_{L_a} = V_{L_b} = \frac{V_{in}}{2L} \tag{2.14}$$

$$\frac{di_{L_a}}{dt} = \frac{di_{L_b}}{dt} = \frac{di_L}{dt} = \frac{V_{in}}{2L} \tag{2.15}$$

$$\frac{di_{V_c}}{dt} = \frac{-V_o}{RC} \tag{2.16}$$

$$A_2 = \begin{bmatrix} 0 & 0 \\ 0 & \frac{-1}{RC} \end{bmatrix} \begin{bmatrix} i_L \\ V_c \end{bmatrix} + \begin{bmatrix} \frac{1}{2L} \\ 0 \end{bmatrix} V_{in} \tag{2.17}$$

2.3.3 Mode 3

$$V_{L_a} = V_{L_b} = \frac{V_{in} - V_o}{2L} \tag{2.18}$$

$$\frac{di_{L_a}}{dt} = \frac{di_{L_b}}{dt} = \frac{di_L}{dt} = \frac{V_{in} - V_o}{2L} \tag{2.19}$$

$$\frac{di_{V_c}}{dt} = \frac{i_L}{C} - \frac{V_o}{RC} \tag{2.20}$$

$$A_3 = \begin{bmatrix} 0 & \frac{-1}{2L} \\ \frac{1}{C} & \frac{-1}{RC} \end{bmatrix} \begin{bmatrix} i_L \\ V_c \end{bmatrix} + \begin{bmatrix} \frac{1}{2L} \\ 0 \end{bmatrix} V_{in} \tag{2.21}$$

By using state space averaging method,

$$A = A_1D_1 + A_2D_2 + A_3(1 - D_1 - D_2) \tag{2.22}$$

$$A = \begin{bmatrix} 0 & \frac{-(1-D_1-D_2)}{2L} \\ \frac{(1-D_1-D_2)}{C} & \frac{1}{RC} \end{bmatrix} \tag{2.23}$$

$$B = B_1D_1 + B_2D_2 + B_3(1 - D_1 - D_2) \tag{2.24}$$

$$B = \begin{bmatrix} \frac{(1+D_1)}{2L} \\ 0 \end{bmatrix} \tag{2.25}$$

The matrices representing the output systems of converter C and D are given in equation 26.

$$y = \begin{bmatrix} 1 & 0 \\ 0 & 1 \end{bmatrix} \begin{bmatrix} i_L \\ V_c \end{bmatrix} + \begin{bmatrix} 0 \\ 0 \end{bmatrix} u \tag{2.26}$$

The steady-state variables can be determined by setting the derivative of the state variable to zero. Consequently, the state space equation becomes equation (27). The average values of the inductor current and output voltage are depicted in equation (28).

$$X = A^{-1} * B * u \tag{2.27}$$

$$X = \begin{bmatrix} i_L \\ V_o \end{bmatrix} = \begin{bmatrix} \frac{V_i n(1+D_1}{R(1-D_1-D_2)^2} \\ \frac{V n(1+D}{(1-D_1-D_2)} \end{bmatrix} \tag{2.28}$$

2.4 Transfer function of the system

2.4.1 Transfer function describing perturbations

Gain relating the change in output voltage to the change in input voltage

$$\frac{\hat{V}_o(S)}{\hat{V}_{in}(S)} = C(SI - A)^{-1}B \tag{2.29}$$

$$\frac{\hat{V}_o(S)}{\hat{V}_{in}(S)} = \frac{(1+D_1)((1-D_1-D_2))}{2LC(S^2 + \frac{S}{RC} + \frac{(1-D_1-D_2)^2}{2LC}} \tag{2.30}$$

2.4.2 Transfer function controlling the system

Change in duty ratio relative to change in output voltage

$$\frac{\hat{V}_o(S)}{\hat{d}(S)} = C(SI - A)^{-1}f \tag{2.31}$$

$$\frac{\hat{V}_o(S)}{\hat{d}(S)} = \frac{\frac{(1+D_1)}{2LC} - \frac{S(1+D_1)(D_1+D_2}{RC(1-D_1-D_2)^2}}{S^2 + \frac{S}{RC} + \frac{(1-D_1-D_2)^2}{2LC})} \tag{2.32}$$

2.5 Efficiency analysis

In this section, the converter efficiency for all the three modes of operation is discussed. r_{L_a} and r_{L_b} are the ESR of the inductors L_a and L_a respectively which is 0.002Ω. Similarly, r_{D_a}, r_{D_b} are the internal resistances and V_{D_a} , V_{D_b} are the voltage drops across the diodes SBR20A300CTB

D_a and D_a, respectively which is 0.014Ω. r_{Q_1} , r_{Q_2} , and r_{Q_3} represent the ON-state resistance of the switches FDP20N40 Q_1 , Q_2 , and Q_3 , respectively which is 0.002Ω. R_o is the load resistance equal to 245Ω.

Mode I: When Q_1 and Q_2 are turned ON and Q_3 is turned OFF.

$$I_c' = -\frac{V_o}{R_o} \tag{2.33}$$

$$V_{L_a}' = V_{in} - i_{L_a}(r_{Q_1} + r_{L_a}) \tag{2.34}$$

Mode II: When Q_1 and Q_2 are turned OFF and Q_3 is turned ON.

$$I_c'' = -\frac{V_o}{R_o} \tag{2.35}$$

$$V_{L_a}'' = \frac{V_{in} - i_{L_a}(r_{Q_3} + r_{L_a} + r_{L_b} + r_{D_a}) - V_{D_a}}{2} \tag{2.36}$$

Mode III: When Q_1 , Q_2 , and Q_3 are turned OFF.

$$I_c''' = I_{L_a} - \frac{V_o}{R_o} \tag{2.37}$$

$$V_{L_a}'' = \frac{V_{in} - V_o - i_{L_a}(r_{L_a} + r_{L_b} + r_{D_b}) - V_{D_b}}{2} \tag{2.38}$$

Applying ampere-second balance principle for the output capacitance C , the following equation is obtained:

$$\int_0^{D_1T_s} I_c' dt + \int_0^{D_2T_s} I_c'' dt + \int_0^{(1-D_1-D_2)T_s} I_c''' dt = 0 \tag{2.39}$$

Simplifying (2.39), the current through the inductor I_{L_a} is obtained as

$$I_{L_a} = \frac{V_o}{R_o(1 - D_1 - D_2)} = \frac{700}{245(1 - 0.5 - 0.35)} = 1904A \tag{2.40}$$

Applying volt-second balance principle on any of the inductor L_a or L_b , the following equation is obtained:

$$\int_0^{D_1T_s} V_{L_a}' dt + \int_0^{D_2T_s} V_{L_a}'' dt + \int_0^{(1-D_1-D_2)T_s} V_{L_a}''' dt = 0 \tag{2.41}$$

Simplifying (2.41), the output voltage is obtained as

$$V_o = \frac{V_{in}(1 + D_1) - (V_{D_a}D_2) - (V_{D_a}(1 - D_1 - D_2)}{\left[\frac{2(1+D_1A_1+D_2A_2+A_3}{R_o(1-D_1-D_2)}\right] + (1 - D_1 - D_2)} \tag{2.42}$$

$$V_o = \frac{70(1 + 0.5) - (70x0.35) - 770(1 - 0.5 - 0.35)}{\left[\frac{2(1+0.5x0.207+0.35x0.1+0.009}{245(1-0.5-0.35)}\right] + (1 - 0.5 - 0.35)} = -221V$$

$$A_1 = r_{Q_1} + (r_{D_a}/2) = 0.2 + (0.014/2) = 0.207 \tag{2.43}$$

$$A_2 = 1/2(r_{D_a} - r_{D_b} + r_{Q_3}) = 1/2(0.014 - 0.014 + 0.2) = 0.1 \quad (2.44)$$

$$A_3 = r_{L_a} + (r_{D_b}/2) = 0.002 + (0.014/2) = 0.009 \quad (2.45)$$

The input and output powers for the proposed converter is obtained as

$$P_{in} = 2V_{in}I_{L_a}D_1 + V_{in}I_{L_a}D_2 + V_{in}I_{L_a}(1 - D_1 - D_2) \quad (2.46)$$

Substituting (2.40) into (2.46), the input power is given as

$$P_{in} = \frac{V_{in}V_o(1 + D_1)}{R_o(1 - D_1 - D_2)} = \frac{70x700(1 + 0.5)}{245(1 - 0.5 - 0.35)} = 2001.63W \quad (2.47)$$

$$P_o = \frac{V_o^2}{R_o} = \frac{700^2}{245} = 2000W \quad (2.48)$$

From (2.42), (2.47), and (2.48), the efficiency of the proposed high gain dc–dc converter (considering only conduction losses) is calculated as

$$\eta = \frac{P_o}{P_{in}} = \frac{V_{in}(1 + D_1) - (V_{D_a}D_2) - (V_{D_a}(1 - D_1 - D_2)}{[\frac{2(1+D_1A_1+D_2A_2+A_3}{R_o(1-D_1-D_1)}] + (1 + D_1)V_{in}} = \frac{2000}{2001.63} = 0.99 \quad (2.49)$$

Due to non ideal values ,output voltage will be less than 700. If hardware is considered then it's efficiency will be in between 95 to 93%.

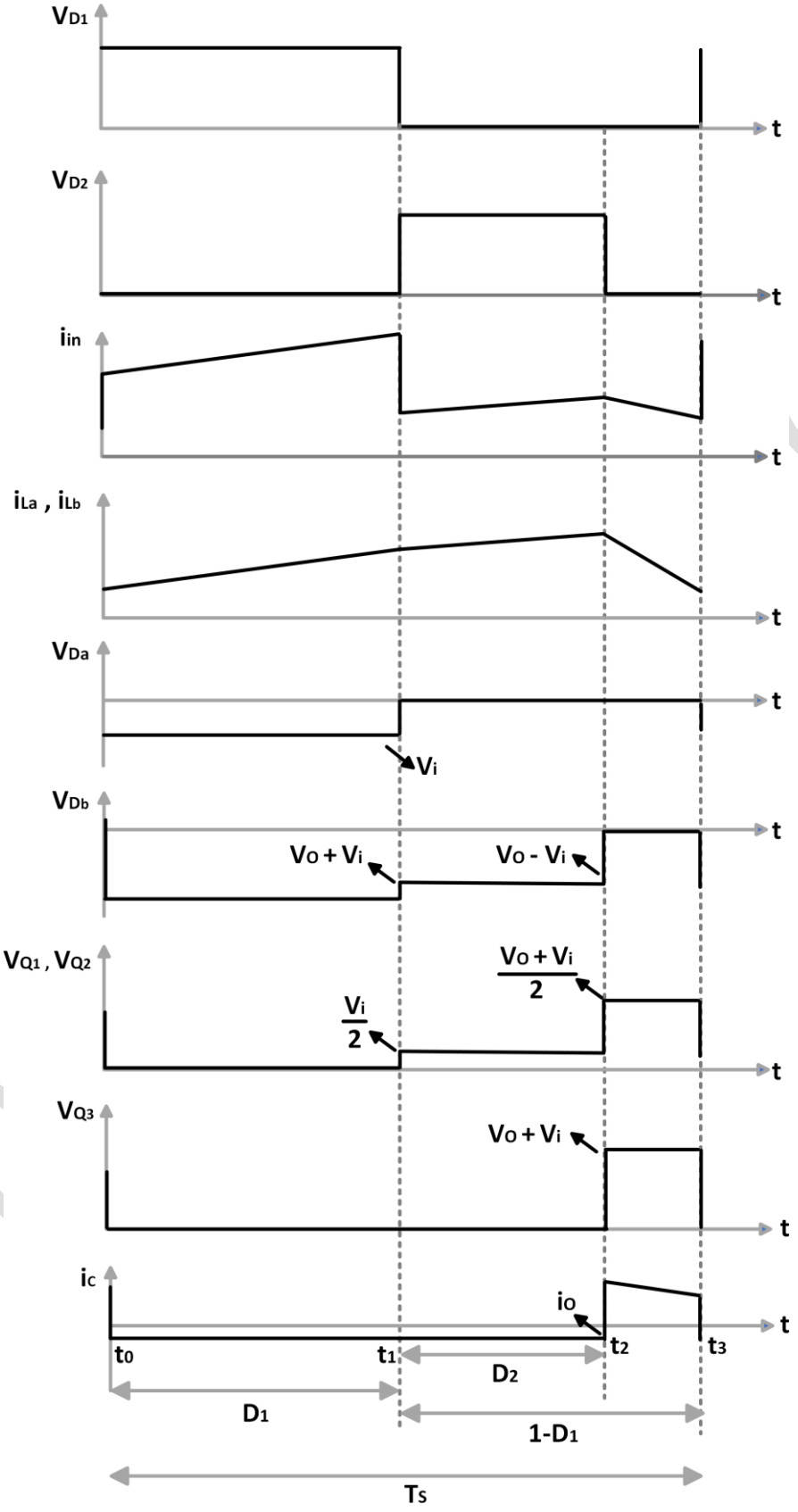

Figure 2.2: Operation of given converter in continuous conduction mode (CCM)

Chapter 3

Proposed System

3.1 Introduction

Solar power is important in power electronics because it's a clean, renewable energy source that can be used to generate electricity. Solar energy doesn't create carbon emissions or greenhouse gases, and it avoids the environmental damage of mining and drilling for fossil fuels. Solar energy is a renewable source of power that can help mitigate climate change. Solar power electronics devices, like inverters, convert direct current (DC) electricity from solar panels into alternating current (AC) electricity for use on the electrical grid. Solar power innovations are improving the efficiency of consumer electronics and making it easier to install advanced industrial systems. Solar power can reduce the electronics industry's environmental impact. Solar panels are becoming more affordable.

An inverter is a power electronic device that takes DC power from an energy source like batteries or solar panels as input and converts it into AC power as output. The AC power generated can be utilized to run electrical appliances and machines that require AC power to function.

Inverters have become indispensable with the rise of renewable energy sources like solar and wind, which generate DC power. They help utilize this DC power for AC applications. Without inverters, DC power from these sources cannot be used directly as most loads are designed for standard AC mains voltage.

The proposed system features a pioneering DC-DC converter specifically designed to harness energy from renewable sources, such as solar panels or wind turbines, and optimize its conversion into usable electricity.

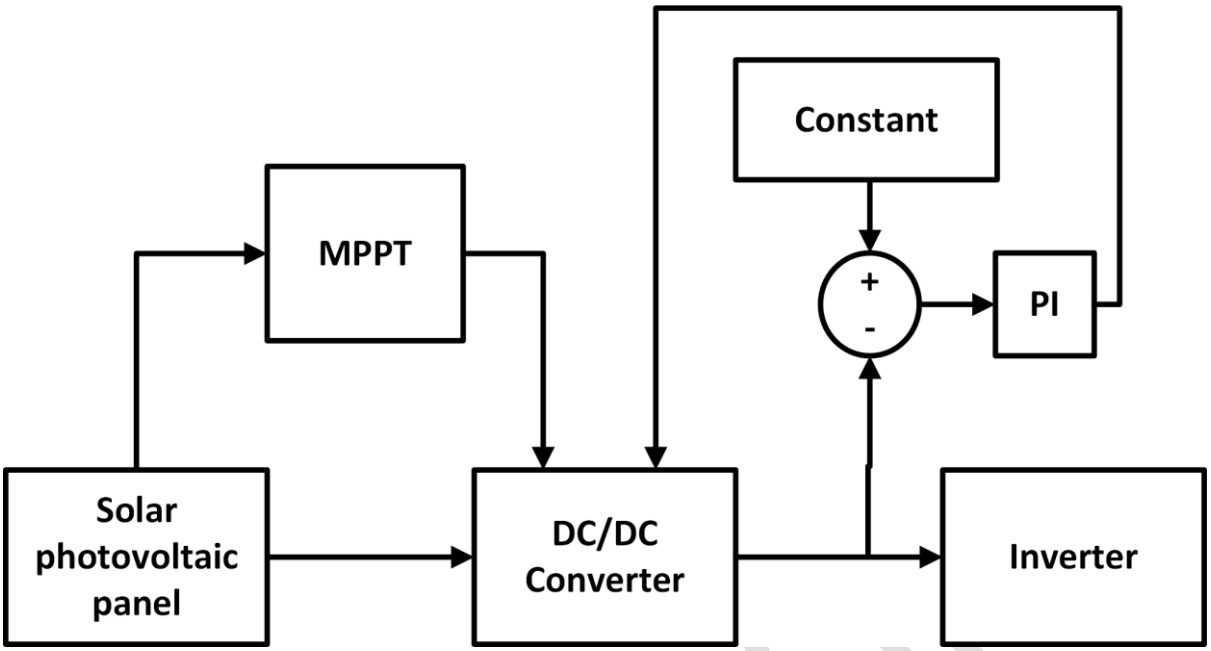

Figure 3.1: Flow diagram of proposed system

Utilizing advanced power electronics and control algorithms, the converter ensures maximum energy extraction and conversion efficiency. As fig. 3.1 suggest the PWM signal is generated by the MPPT algorithm and is subsequently directed to switch 1 and switch 2. Within the closed-loop system, the output voltage is compared with the desired output voltage, and PWM signals are generated accordingly. These generated PWM signals are then applied to switch 3. In Table I the values of selected parameters are given.

- Sunlight: The solar panel absorbs sunlight and generates DC electricity.
- MPPT: The MPPT controller monitors the panel's output and adjusts its load impedance to maximize power generation.
- DC/DC Converter: The converter boosts the DC voltage to a suitable level for the inverter.
- PI Controller: The PI controller regulates the output voltage of the DC/DC converter to maintain a constant value.
- Inverter: The inverter converts the DC voltage into AC voltage, which can be used to power loads.

Fig. 3.2 shows the circuit diagram of proposed system.

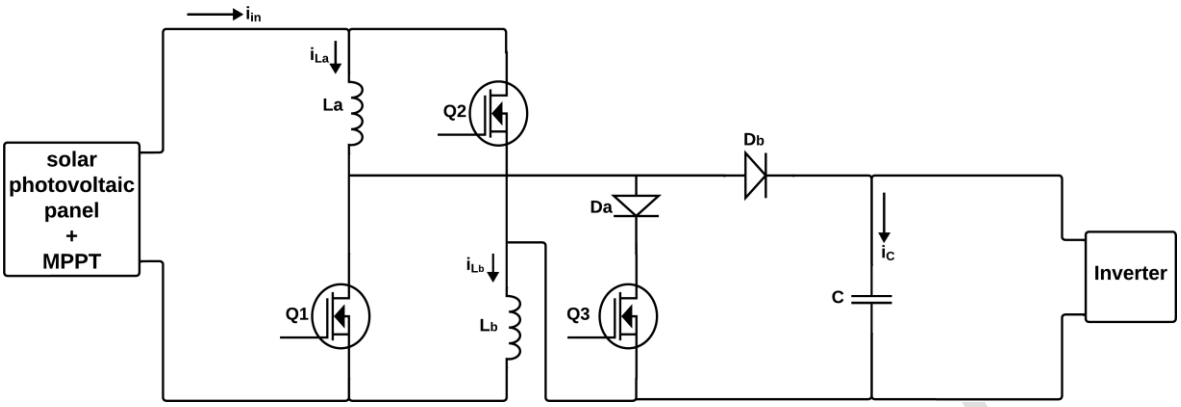

Figure 3.2: Circuit diagram of proposed system

3.2 Operation of proposed system

Further explanation is provided regarding the operational modes of the converter.

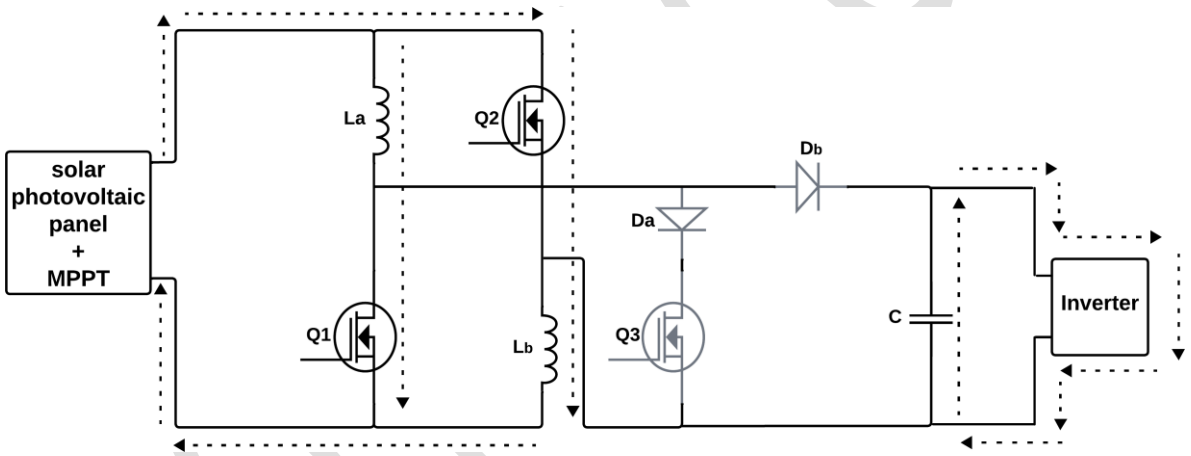

Figure 3.3: Mode 1

Mode I: Q_1 and Q_2 are activated while Q_3 is deactivated. Flow of current shown in fig. 3.3. Energy from the source is conveyed to inductors L_a and L_b, while the stored energy in capacitor C is released to the load. During this phase, diodes D_a and D_b remain in a reverse bias state.

Mode II: Q_1 and Q_2 are deactivated while Q_3 is activated. The current pathway during this interval is illustrated in fig. 3.4. Energy from the source is conveyed to the inductors, and the current passes through L_a, D_a, and L_b. When diode D_b stays in reverse bias, the energy stored in capacitor C is transferred to the load.

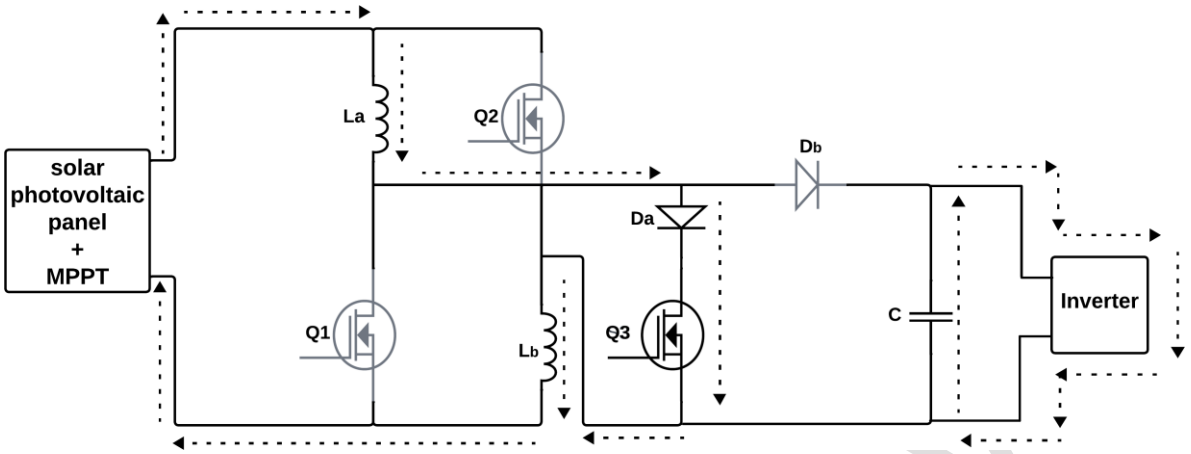

Figure 3.4: Mode 2

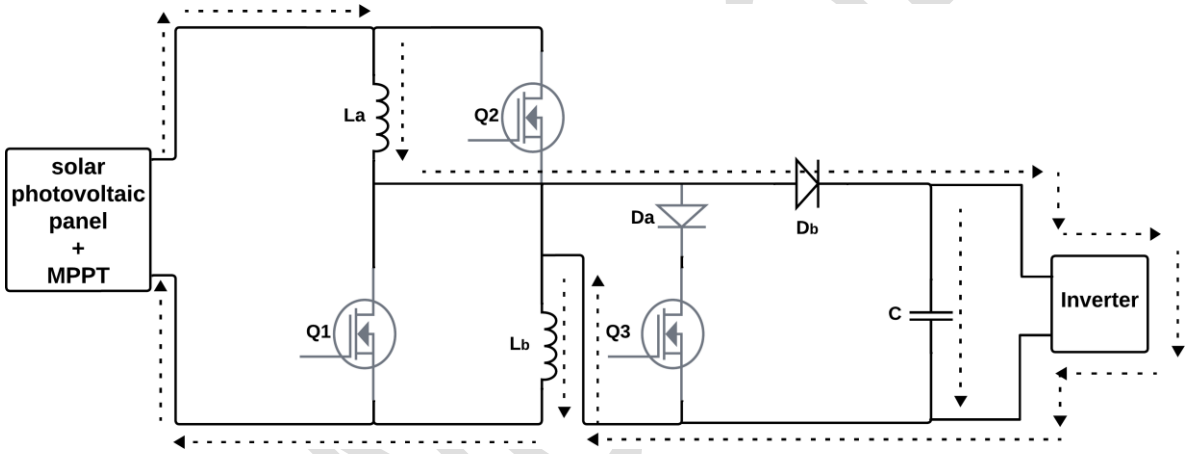

Figure 3.5: Mode 3

Mode III: Q_1, Q_2, and Q_3 are deactivated. The current flow in the circuit is shown in fig. 3.5. In this operational state, both the source and the inductors provide power to the load. Diode D_a is under reverse bias conditions. Furthermore, capacitor C is in the process of charging as diode D_b is forward biased.

Simulation selection is a critical step in the modeling and analysis of complex systems. It involves choosing the most appropriate simulation method to represent the system's behavior and achieve the desired research objectives.

- **Rated Power (Po):** This is the maximum power output that the inverter can deliver, which is 2000W in this case.

- **Input Voltage (Vin):** This is the voltage at the input of the inverter, which is 70V. This

voltage is likely from a DC source, such as a battery or solar panel.

- **Output Voltage (Vo):** This is the voltage at the output of the inverter, which is 700V. This voltage is typically an AC voltage that can be used to power various loads.
- **Duty Ratio (D1, D2):** These are parameters that determine the on-time of the switching devices (MOSFETs) in the inverter. D1 and D2 are 0.5 and 0.35, respectively.
- **Switching Frequency:** This is the frequency at which the switching devices are turned on and off. It is 50kHz in this case.
- **Inductor (La, Lb):** These are inductors used in the inverter to filter the output voltage and reduce ripple. La and Lb are both 1.75mH.
- **Capacitor (C):** This is a capacitor used in the inverter to filter the output voltage and reduce ripple. C is 3.99 μF.
- **Power MOSFETs (Q1, Q2, Q3):** These are the switching devices in the inverter. There are 3 MOSFETs.
- **Diodes (Da, Db):** These are diodes used in the inverter to allow current to flow in one direction only. There are 2 diodes.

3.3 MATLAB Simulation

A simulation of DC/DC converter powered by solar photovoltaic panels and subsequently transformed into AC using an inverter is created in MATLAB/SIMULINK as shown in fig. 3.6. This system finds application in various industrial automation scenarios, where it is utilized for tasks such as power conditioning, motor control, and voltage conversion. In a closed-loop configuration, a PI controller is employed to regulate the PWM signal, ensuring it provides suitable outputs.

3.3.1 Analysis of Duty ratio

The Table II illustrates variations in output voltage, output power, and efficiency of a device, likely a DC-DC converter, across different duty ratios. In fig. 3.7 duty ratios, ranging from

Table 3.1: Simulation Selection

Parameters	Values
Rated Power P_o	2000W
Input Voltage V_{in}	70V
Output Voltage V_o	700V
Duty Ratio D_1	0.5
Duty Ratio D_2	0.35
Switching Frequency	50kHz
Inductor L_a, L_b	1.75mH
Capacitor C	3.99μF
Power MOSFET Q_1, Q_2, Q_3	3
Diodes D_a, D_b	2

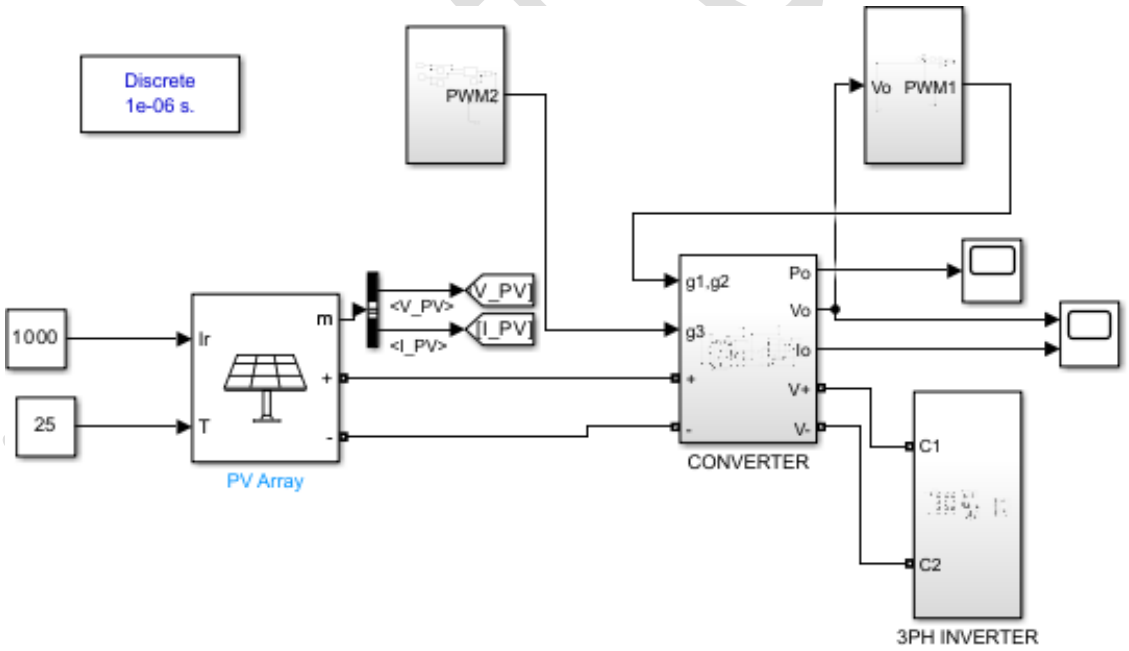

Figure 3.6: Simulation of proposed system

0.45 to 0.7, are displayed on the x-axis. The y-axis denotes output voltage, output power, and efficiency, respectively. The provided plot shows the relationship between the duty ratio D1 and the output voltage, output power, and efficiency of a power electronics circuit.

Table 3.2: Duty Ratio 1 fluctuates

Duty Ratio 1	Duty Ratio 2	Output Voltage	Output Current	Output Power	Efficiency
0.45	0.35	554.8	2.264	1256	62.8
0.5	0.35	699.7	2.856	1998	99.9
0.55	0.35	707.1	2.886	2041	99.7
0.6	0.35	707.5	2.888	2043	99.5
0.65	0.35	699.6	2.855	1998	98.3
0.7	0.35	686.5	2.802	1924	96.2

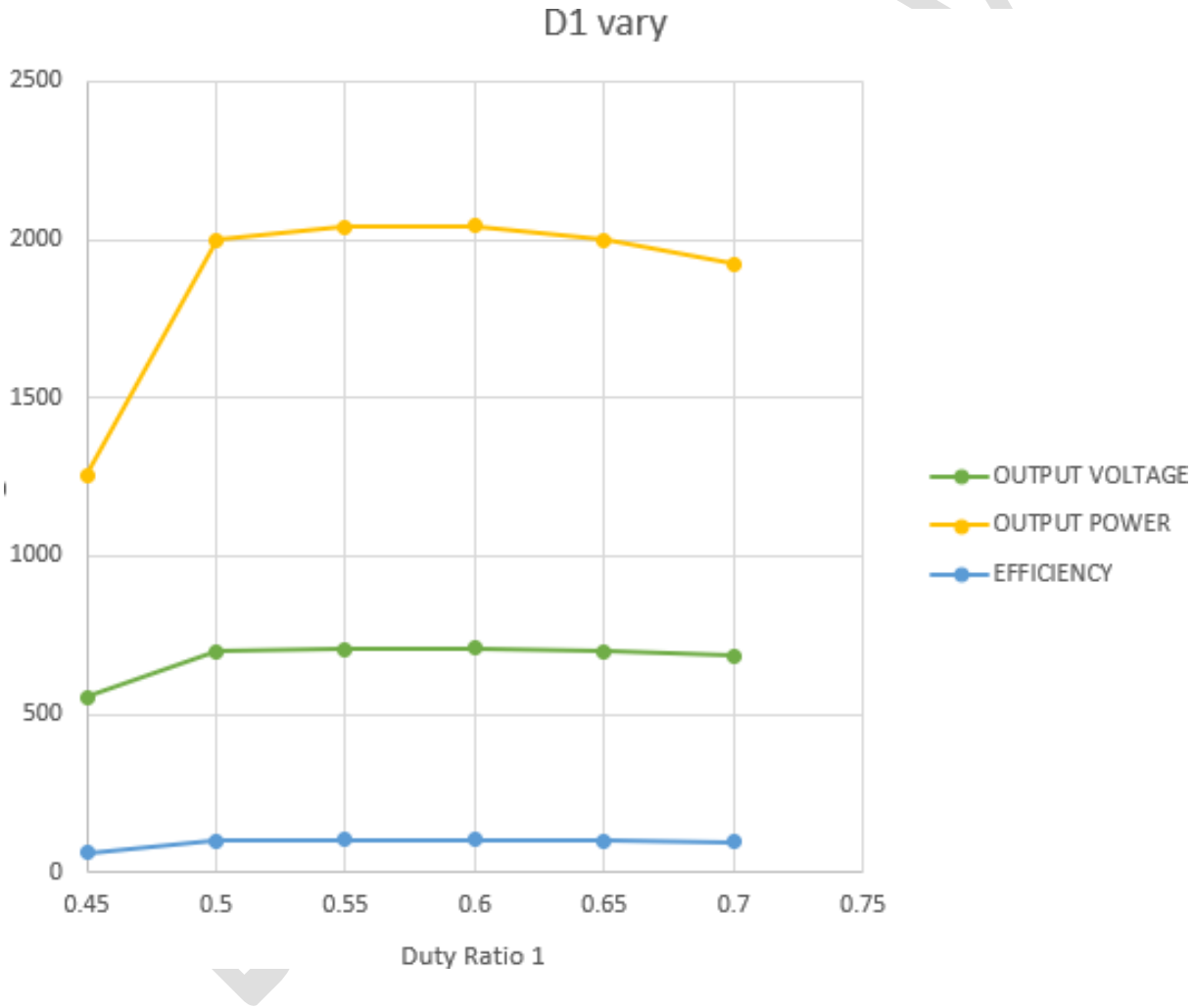

Figure 3.7: Effects on several parameters When duty ratio 1 is varied while duty ratio 2 remains fixed

Output Voltage: As D1 increases, the output voltage also increases. This is because D1 controls the on-time of the switching device, which directly affects the average voltage applied to the load.

Output Power: The output power initially increases with D1, reaches a maximum point,

and then starts to decrease. This is because there is a trade-off between conduction losses and switching losses. At low D1, conduction losses are high, while at high D1, switching losses are high. The optimal D1 value maximizes the output power by minimizing the combined losses.

Efficiency: The efficiency initially increases with D1, reaches a maximum point, and then starts to decrease. This is similar to the output power trend, as efficiency is directly related to the ratio of output power to input power.

The plot demonstrates the importance of selecting an appropriate D1 value to optimize the performance of the power electronics circuit. By carefully considering the trade-offs between output voltage, output power, and efficiency, the optimal D1 value can be determined to achieve the desired operating characteristics.

Observations suggest that the device's efficiency peaks around a duty ratio of approximately 0.35 and 0.5, coinciding with the highest point on the blue line.

The Table III illustrates variations in output voltage, output power, and efficiency of a device, likely a DC-DC converter, across different duty ratios. In fig. 3.8. duty ratios, ranging from 0.3 to 0.55, are displayed on the x-axis. The y-axis denotes output voltage, output power, and efficiency, respectively.

The provided plot shows the relationship between the duty ratio D2 and the output voltage, output power, and efficiency of a power electronics circuit.

Table 3.3: Duty Ratio 2 fluctuates

Duty Ratio 1	Duty Ratio 2	Output Voltage	Output Current	Output Power	Efficiency
0.5	0.3	572.4	2.336	1337	66.85
0.5	0.35	699.7	2.856	1998	99.9
0.5	0.4	558.3	2.279	1272	63.6
0.5	0.45	302.1	1.233	372.5	18.62
0.5	0.5	5.361	0.021	0.117	0.005
0.5	0.55	5.401	0.022	0.119	0.005

Output Voltage: As D2 increases, the output voltage decreases. This is because D2 controls the on-time of the switching device in a way that reduces the average voltage applied to the load. Output Power: The output power initially increases with D2, reaches a maximum point, and then starts to decrease rapidly. This is likely due to increased switching losses and reduced conduction losses. Efficiency: The efficiency initially increases with D2, reaches a maximum point, and then starts to decrease rapidly. This is similar to the output power trend, as efficiency

is directly related to the ratio of output power to input power.

The plot demonstrates the importance of selecting an appropriate D2 value to optimize the performance of the power electronics circuit. By carefully considering the trade-offs between output voltage, output power, and efficiency, the optimal D2 value can be determined to achieve the desired operating characteristics. It's important to note that the specific behavior of the circuit may vary depending on the design and operating conditions.

Observations suggest that the device's efficiency peaks around a duty ratio of approximately 0.5 and 0.35, coinciding with the highest point on the blue line.

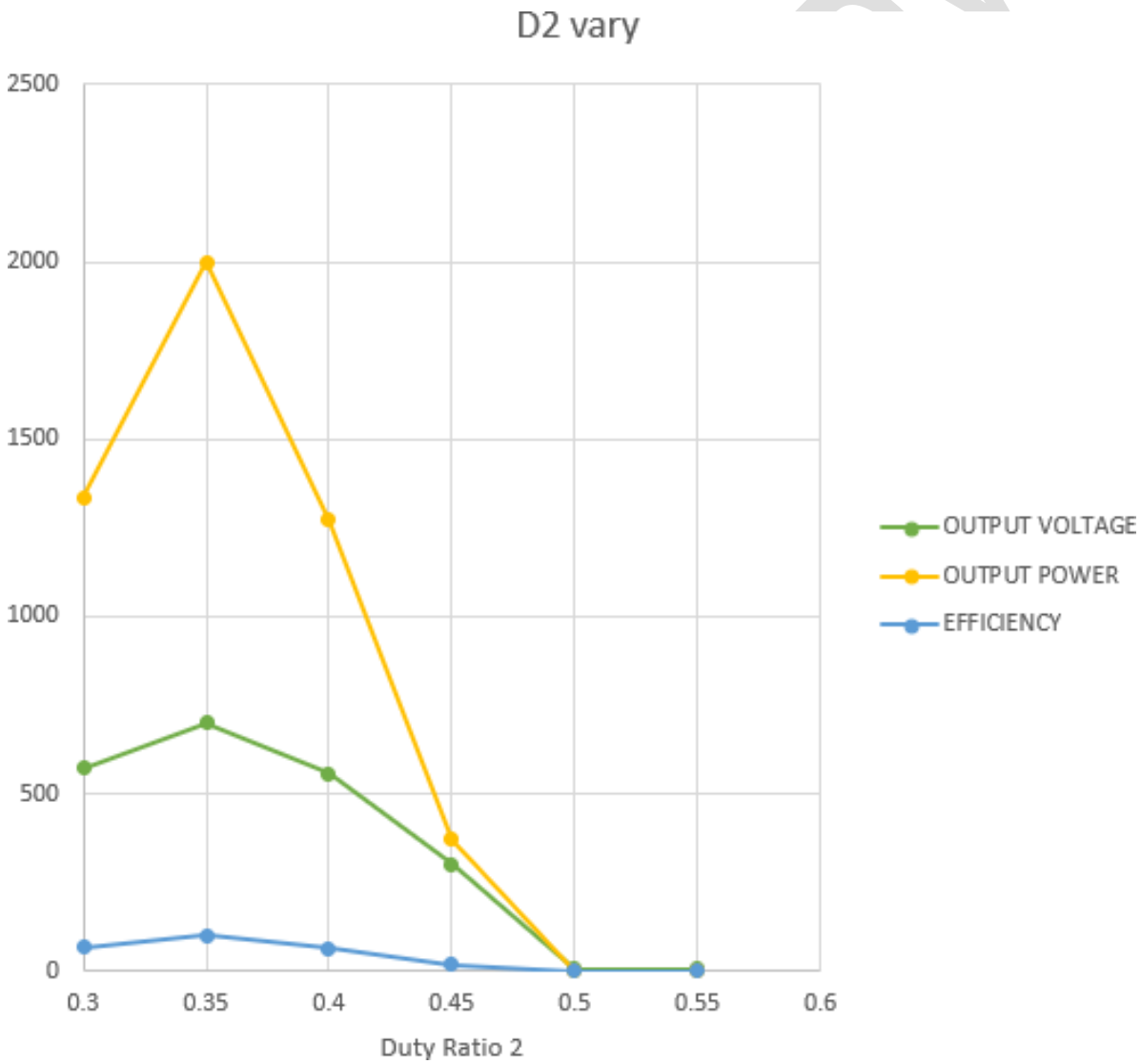

Figure 3.8: Effects on several parameters When duty ratio 2 is varied while duty ratio 1 remains fixed

Chapter 4

Simulation Results

4.1 Introduction

A real-time simulation environment is a platform that lets users interact with and analyze systems in real time. It synchronizes with actual time, providing immediate feedback and supporting real-time decision-making.These environments offer instant monitoring and adjustment capabilities.Operating in real time is essential for modern technological advancement and operational strategy, significantly enhancing safety, productivity, and responsiveness across diverse industries.

MATLAB/ Simulink serves as a powerful platform for real-time simulation and testing. Simulink, known for its user-friendly graphical interface, enables users to accurately model, simulate, and analyze complex dynamic systems.

4.2 Comparision of Conveters

Table 4.1 provides a comparative analysis of various power electronic converters. The parameters considered include the voltage gain, number of MOSFETs, diodes, inductors, and capacitors used in each converter.

Proposed Converter: This is likely a new or innovative converter design being introduced.

Conventional Boost Converter: A well-established type of DC-DC converter used to step up the input voltage.

Converter in [8] and [9]: These refer to converters described in specific research papers.

Table 4.1: Comparision of Different Converters

Parameters	Proposed Converter	Conventional Boost Converter	Converter in [8]	Converter in [9]
Voltage Gain	$\frac{1+D_1}{1-D_1-D_2}$	$\frac{1}{1-D}$	$\frac{1+D}{1-D}$	$\frac{1+D}{1-D}$
Voltage stress on switches	$V_{Q_1} = V_{Q_2} = \frac{V_o+V_{in}}{2} = 385V$ $V_{Q3} = V_o = 700V$	$V_o = 700V$	$V_{Q_1} = V_{Q_2} = \frac{V_o+V_{in}}{2} = 385V$	$V_{Q_1} = V_{Q_2} = \frac{V_o+V_{in}}{2} = 385V$ $V_{Q3} = V_o + V_{in} = 770V$
Voltage stress on diodes	$V_{Da} = V_{in} = 70V$ $V_{Db} = V_{in} + V_o = 770V$	$V_o = 700V$	$V_D = V_o + V_{in} = 770V$	-
No. of MOSFETs	3	1	2	3
No. of Diodes	2	1	1	0
No. of Inductors	2	1	2	2
No. of Capacitors	1	1	1	1

4.3 Steady-state Characteristics

Steady-state in a power converter refers to the condition where the input and output variables of the converter have reached a constant, unchanging state over time. This is typically achieved after the converter has been operating for a sufficient period. The value that the system output (such as voltage, current, or temperature) stabilizes at after the transient effects have decayed. A constant input voltage to a converter and measure the steady-state output voltage, the steady-state gain tells you how efficiently the system converts the input to the output.

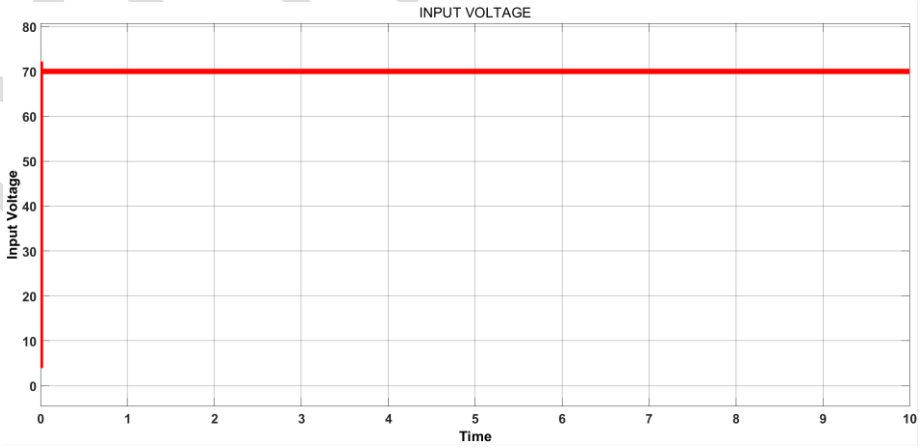

Figure 4.1: INPUT VOLTAGE

Fig. 4.1 displays the input voltage originating from a renewable source, specifically a solar photovoltaic panel, with a value of 70V.

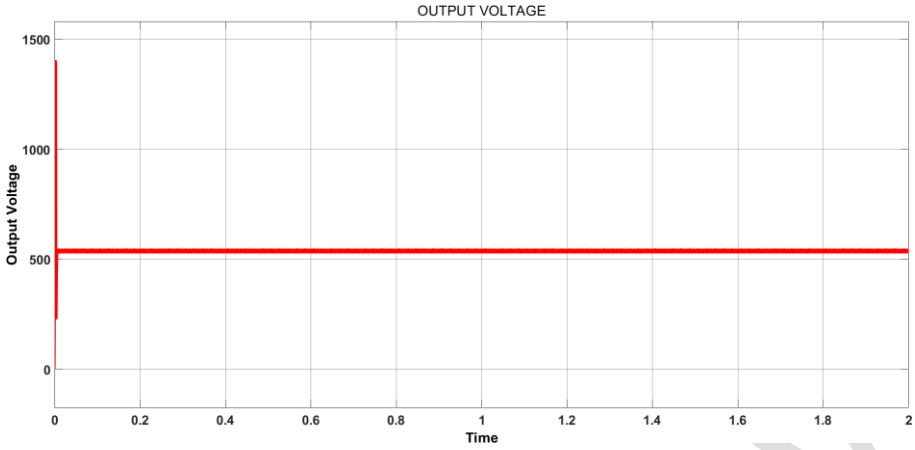

Figure 4.2: OUTPUT VOLTAGE

Fig. 4.2 illustrates the output voltage and current of the converter when connected to an inverter. The expected output voltage is 700V, assuming a voltage gain of 10.

However, when the inverter is connected, the increased load leads to a voltage drop, with the output voltage falling to 549V.

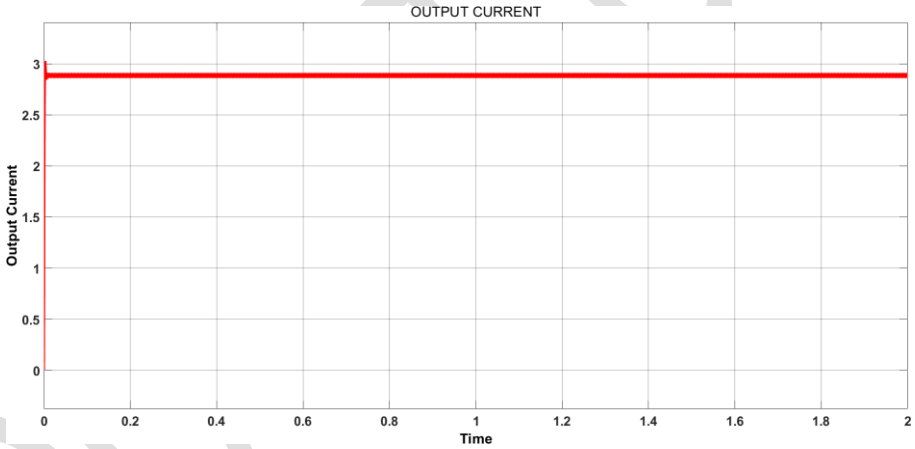

Figure 4.3: OUTPUT CURRENT

Fig. 4.3 indicates that the output current of given converter is 2.857A.

A lower current typically leads to higher system efficiency because it reduces the power losses in the system, particularly in the components like wires and semiconductors that tend to lose more energy at higher currents. In essence, by operating at a lower current, the converter minimizes these losses, allowing more of the input energy to be converted into useful output power rather than being wasted as heat. This results in improved overall efficiency of the system.

Fig. 4.4 displays the output power of the given converter, which closely matches the input

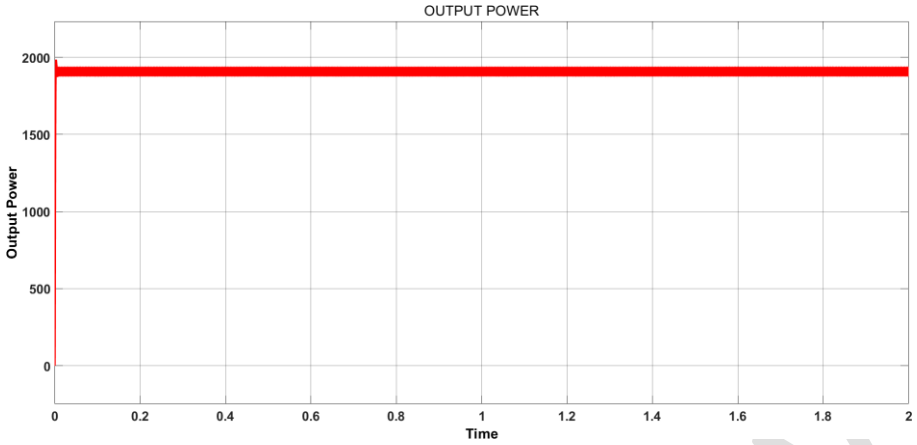

Figure 4.4: OUTPUT POWER

power as expected, achieving an efficiency of 99%.

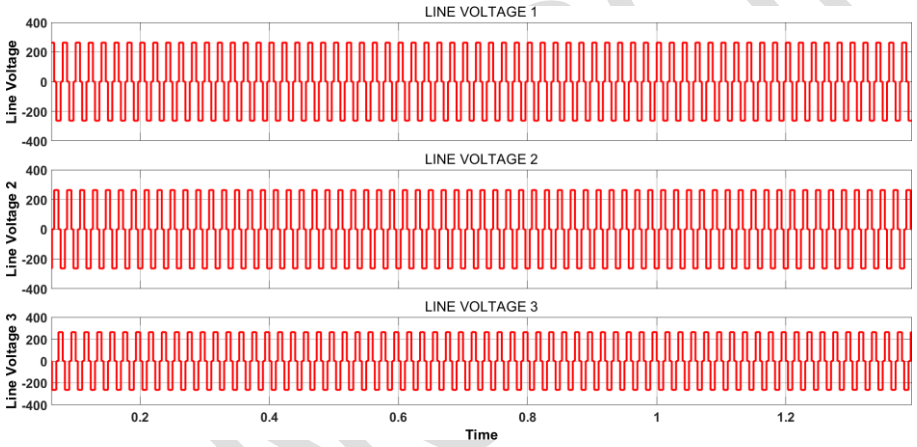

Figure 4.5: LINE VOLTAGES

Fig. 4.5 illustrates the inverter output, which is a line voltage of 274.5V. This output is expected to be half of the converter's output voltage.

Chapter 5

Conclusion and Future Scope

5.1 Conclusion

This paper introduces a non-isolated DC-DC converter for high gain designed to attain a high voltage gain. The converter offers significant advantages through the incorporation of switch Q_3 and the working of three switches with two distinct duty ratios. Theoretical analysis was conducted to assess parameters such as voltage gain, efficiency, and voltage stress on switches and diodes for this converter. This paper presents a technique for the smooth interfacing of renewable energy sources to the AC grid. A closed-loop control strategy is implemented in this paper to regulate variations in output voltage. This system is suitable for AC power grids applications with a capacity of 2KW. By utilizing a renewable energy source, it offers an environmentally friendly solution, decreasing reliance on fossil fuels and reducing greenhouse gas emissions. Future work could focus on integrating energy storage with this system.

5.2 Future Scope

The future scope of non-isolated high gain DC-DC converters interfacing renewables and the AC grid is promising, given the increasing adoption of renewable energy systems and the need for efficient energy conversion. Some key areas of future development include:

- Developing advanced control strategies, such as digital and predictive control, will optimize the converter's performance and ensure better dynamic response.
- Non-isolated high gain DC-DC converters are essential in integrating renewables, partic-

ularly in photovoltaic (PV) and wind energy systems. Future work will focus on maximizing power extraction even under varying environmental conditions.

- As grids become smarter, non-isolated DC-DC converters will need to be more adaptive, supporting bidirectional power flow and seamless connection to both microgrids and the main grid.
- With high power densities and fast switching frequencies, future converters need to minimize grid harmonics, improving power quality and reducing electromagnetic interference (EMI).

Bibliography

[1] N. Eghtedarpour and E. Farjah, “Distributed charge/discharge control of energy storages in a renewable-energy-based DC micro-grid,” IET Renewable Power Gener., vol. 8, no. 1, pp. 45–57, Jan. 2014.

[2] J.M.Carrasco etal., “Power-electronic systems for the grid integration of renewable energy sources: A survey,” IEEE Trans. Ind. Electron., vol. 53, no. 4, pp. 1002–1016, Jun. 2006.

[3] B. Bryant and M. K. Kazimierczuk, “Voltage-loop power-stage transfer functions with MOSFET delay for boost PWM converter operating in CCM,”IEEETrans.Ind. Electron., vol. 54, no. 1, pp. 347–353, Feb. 2007.

[4] X.Wu,J.Zhang,X.Ye,andZ.Qian,“Analysisandderivationsforafamily ZVS converter based on a new active clamp ZVS cell,” IEEE Trans. Ind. Electron., vol. 55, no. 2, pp. 773–781, Feb. 2008.

[5] F. L. Tofoli, D. d. C. Pereira, W. Josias de Paula, and D. d. S. Oliveira J´ unior, “Survey on non-isolated high-voltage step-up dc–dc topologies based on the boost converter,” IET Power Electron., vol. 8, no. 10, pp. 2044–2057, Oct. 2015.

[6] M. A. Abusara, J. M. Guerrero, and S. M. Sharkh, “Line-interactive UPS for microgrids,” IEEE Trans. Ind. Electron., vol. 61, no. 3, pp. 1292–1300, Mar. 2014.

[7] M.YilmazandP.T.Krein,“Reviewofbatterychargertopologies,charging power levels, and infrastructure for plug-in electric and hybrid vehicles,” IEEE Trans. Power Electron., vol. 28, no. 5, pp. 2151–2169, May 2013.

[8] L. S. Yang, T. J. Liang, and J. F. Chen, “Transformerless DC–DC converters with high step-up voltage gain,” IEEE Trans. Ind. Electron., vol. 56, no. 8, pp. 3144–3152, Aug. 2009.

[9] L. S. Yang and T. J. Liang, “Analysis and implementation of a novel bidirectional DC–DCconverter,”IEEETrans.Ind.Electron.,vol.59,no.1, pp. 422–434, Jan. 2012.

[10] A. Ajami, H. Ardi, and A. Farakhor, “A novel high step-up DC/DC converter based on integrating coupled inductor and switched-capacitor techniques for renewable energy applications,” IEEE Trans. Power Electron., vol. 30, no. 8, pp. 4255–4263, Aug. 2015.

[11] S. M.Chen,M.L.Lao,Y.H.Hsieh,T.J. Liang, and K. H. Chen, “Anovel switched-coupled-inductor DC–DC step-up converter and its derivatives,” IEEE Trans. Ind. Appl., vol. 51, no. 1, pp. 309–314.

[12] M.Forouzesh, K. Yari, A. Baghramian, and S. Hasanpour, “Single-switch high step-up converter based on coupled inductor and switched capacitor techniques with quasi-resonant operation,” IET Power Electron., vol. 10, no. 2, pp. 240–250, Oct. 2017.

[13] L. H. S. C. Barreto, E. A. A. Coelho, V. J. Farias, J. C. de Oliveira, L.C. de Freitas, and J. J. Batista Vieira, “A quasi-resonant quadratic boost converter using a single resonant network,” IEEE Trans. Ind. Electron., vol. 52, no. 2, pp. 552–557, Apr. 2005.

[14] F. L. Tofoli, D. d. C. Pereira, W. Josias de Paula, and D. d. S. Oliveira J´ unior, “Survey on non-isolated high-voltage step-up dc–dc topologies based on the boost converter,” IET Power Electron., vol. 8, no. 10, pp. 2044–2057, Oct. 2015.

[15] A. Elserougi, S. Ahmed, and A. Massoud, “High voltage pulse generator based on DC-to-DC boost converter with capacitor-diode voltage multi pliers for bacterial decontamination,” in Proc. 41st Annu. Conf. IEEE Ind. Electron. Soc., Yokohama, Japan, 2015, pp. 000322–000326.

[16] Y. Zhao, W. Li, Y. Deng, and X. He, “High step-up boost converter with passive lossless clamp circuit for non-isolated high step-up applications,” IET Power Electron., vol. 4, no. 8, pp. 851–859, Sep. 2011.

[17] M. H. Rashid, Power Electronics Handbook: Devices, Circuits, and Applications. New York, NY, USA: Academic, 2007, ch. 13, pp. 245–259.

[18] B. Axelrod, Y. Berkovich, and A. Ioinovici, “Switched-capacitor/switched-inductor structures for getting transformerless hybrid DC–DC PWM converters,” IEEE Trans. Circuits Syst. I, Reg. Papers, vol. 55, no. 2, pp. 687–696, Mar. 2008.

[19] K. D. Kim, J. G. Kim, Y. C. Jung, and C. Y. Won, “Improved non-isolated high voltage gain boost converter using coupled inductors,” in Proc. Int. Conf. Elect. Mach. Syst., Beijing, China, 2011, pp. 1–6.

[20] S. Dwari and L. Parsa, “An efficient high-step-up interleaved DC–DC converter with a common active clamp,” IEEE Trans. Power Electron., vol. 26, no. 1, pp. 66–78, Jan. 2011.

[21] M. Lakshmi and S. Hemamalini, "Nonisolated High Gain DC–DC Converter for DC Microgrids," in IEEE Transactions on Industrial Electronics, vol. 65, no. 2, pp. 1205-1212, Feb. 2018, doi: 10.1109/TIE.2017.2733463.